

Electrooxidation of ethylene glycol on Pt-based catalysts dispersed in polyaniline

A. KELAIDOPOULOU*, E. ABELIDOU*, A. PAPOUTSIS*, E. K. POLYCHRONIADIS‡, G. KOKKINIDIS*

*Laboratory of Physical Chemistry, Department of Chemistry and ‡Solid State Physics Section, Department of Physics, Aristotle University of Thessaloniki, 54006 Thessaloniki, Greece

Received 2 October 1997; accepted in revised form 10 December 1997

Platinum dispersed in a polyaniline film is a better catalyst than smooth Pt for ethylene glycol electrooxidation in perchloric acid aqueous solutions. The catalytic activity of the platinum micro-particles is further enhanced when Ru, Sn or both are codeposited. The PANi/Pt–Sn assembly shows the highest electrocatalytic activity of the electrodes examined. Underpotential deposition of Tl and Bi on dispersed Pt inhibits EG electrooxidation while Pb causes significant catalysis only with a specific preparation method electrocatalyst. The morphology and the identity of the metallic dispersion is examined by transmission electron microscopy.

Keywords: *electrooxidation, ethylene glycol, Pt-based catalysts, polyaniline*

1. Introduction

The possibility of using ethylene glycol (EG) as a liquid fuel directly oxidized on platinum in a fuel cell makes the study of its electrooxidation important. It is well known that using such a fuel the performance of the anode material, which is usually Pt, falls over a short length of time due to the formation of contaminating intermediates which adsorb onto the catalyst surface blocking further action. A method of preventing platinum poisoning and enhancing its catalytic activity is modification by adatoms deposited at underpotential [1–3] and the use of platinum-based multimetallic systems [4–8]. Even more efficient electrocatalysts can be obtained by dispersing Pt or Pt-metal codeposits in conducting polymer supports. Such modified electrodes have been successfully used for the oxidation of small organic molecules [9–24], i.e. methanol, formic acid, formaldehyde or even the reduction of oxygen, and the generation and oxidation of hydrogen. The conducting polymers which are mostly used in these studies are poly(4-vinylpyridine) cross linked or linear, polyvinylacetic acid, polyaniline, polypyrrole, polythiophene and derivatives.

The electrooxidation of EG on platinum has been much researched, but its mechanism is still not completely understood. According to the literature [25, 26], a number of intermediate steps take place and lead to the formation of several products; glycolaldehyde, glyoxal, glycolic acid, glyoxylic acid and oxalic acid. Some paths, however, involve rupture of the C–C bond thus producing C₁ molecules like formaldehyde and formic acid [3]. Further oxidation of all the intermediates produces CO₂.

In this work, we report the electrooxidation of EG on pure and modified platinum electrodes incorpo-

rated in the form of microparticles in a polyaniline matrix in aqueous acidic solutions. Polyaniline (PANi) was chosen as the host polymer because of its stability as well as its porosity and relatively high electrical conductivity. For the modification of platinum two methods were adopted. Underpotential deposition of heavy metals (Pb, Tl and Bi) and codeposition of Pt with one or two secondary metals (Ru, Sn, Ru and Sn, Pb). Transmission electron microscopy was employed to provide information about the morphology and the identity of the deposited electrocatalyst particles.

2. Experimental details

A glassy carbon disc, a glassy carbon rotating disc (EDI 101T from Tacussel) and a platinum bead were the working electrodes employed. Before each experiment, the disc electrodes were mechanically polished using emery paper and electrochemically activated using preelectrolysis. The platinum bead was first pretreated by flame and then electrochemically activated. The modification of the disc electrodes was performed in two steps: (a) electropolymerisation of aniline by potential cycling ($v = 50 \text{ mV s}^{-1}$) between 0 and 0.98 V vs SHE in a 0.5 M H₂SO₄ + 0.1 M aniline aqueous solution [27], (b) electrodeposition of the metallic particles potentiostatically at 0.1 V vs SHE.

The thickness of the polymer film was estimated from the first anodic peak height of the cyclic voltammogram of polyaniline in base electrolyte solution (aqueous H₂SO₄ 0.5 M) [28]. The polymer film used was 0.5 μm thick unless otherwise stated.

For platinum deposition the solution employed was 0.5 M H₂SO₄ + 2×10^{-4} M K₂PtCl₆. For the

codepositions the solutions also contained 1×10^{-4} M $\text{RuCl}_3 + 2 \times 10^{-4}$ M HCl for the case of Pt–Ru, 1.5×10^{-4} M $\text{NH}_4[\text{SnCl}_3] + 3 \times 10^{-4}$ M HCl for Pt–Sn, 1×10^{-4} M $\text{RuCl}_3 + 1.5 \times 10^{-4}$ M $\text{NH}_4[\text{SnCl}_3] + 5 \times 10^{-4}$ M HCl for Pt–Ru–Sn and 1×10^{-4} M $\text{H}[\text{PbCl}_3] + 0.2$ M NaCl for Pt–Pb. The mass of the metal or metals incorporated was calculated from the charge passed considering that platinum was the only metal deposited. After each experiment polyaniline with the incorporated metallic microparticles was removed from the electrode surface by dissolution in chromic + sulphuric acid. The cell used for the voltammetric study of EG was double walled and thermostated at 25 ± 0.1 °C. A $\text{Hg}/\text{Hg}_2\text{SO}_4/\text{Na}_2\text{SO}_4$ (sat.) electrode, connected to the cell by a Luggin capillary, and a Pt sheet served as the reference and the counter electrode, respectively. The solutions were thoroughly deoxygenated by purging the cell system with ultrapure nitrogen. Electrode potentials are given on the standard hydrogen electrode (SHE) scale.

Solutions were prepared using triply distilled water and reagents from Merck ('suprapur' for HClO_4 and H_2SO_4 , GR for HCl , PbCO_3 and for RuCl_3 , extra-pure for Bi_2O_3), Fluka (puriss. for K_2PtCl_6 and aniline), Alfa inorganics ($\text{NH}_4[\text{SnCl}_3]$), Carlo Erba (RP Ti_2CO_3) and Prolabo (*zur Analyse* ethylene glycol). Before each experiment aniline was purified by distillation.

The electronic set-up consisted of a homemade potentiostat, a voltage scan generator (Wenking VSG 72), a double pulse control generator (Wenking DPC 72) and a 3023 X–Y recorder from Yokogawa. For the transmission electron microscopy (TEM) observations Au (300 mesh) grids supplied by Agar Scientific Ltd were used. The grids were activated by applying a continuous sweep ($v = 1 \text{ V s}^{-1}$) between hydrogen evolution and just before oxygen evolution in 0.1 M HClO_4 solution until the cyclic voltammograms (0.1 V s^{-1}) obtained the known shape for Au. The TEM study was performed with a Joel 100CX microscope operating at 120 kV.

3. Results and discussion

3.1. EG electrooxidation on smooth Pt and Pt dispersed in polyaniline

Figure 1 shows the voltammogram of a platinum bead in a perchloric acid aqueous solution containing EG. The onset of its electrooxidation during the positive sweep appears within the double layer region; at 0.5 V. The main oxidation peak is relatively wide and reaches a maximum of 0.45 mA cm^{-2} at 0.75 V for a scan rate of 5 mV s^{-1} . An oxidation peak also appears during the reverse sweep. It commences immediately after the onset of oxide reduction indicating the typical behaviour of the electrochemical oxidation of organic compounds on platinum, for which the reaction requires oxide-free sites to take place. The current density of the maximum is

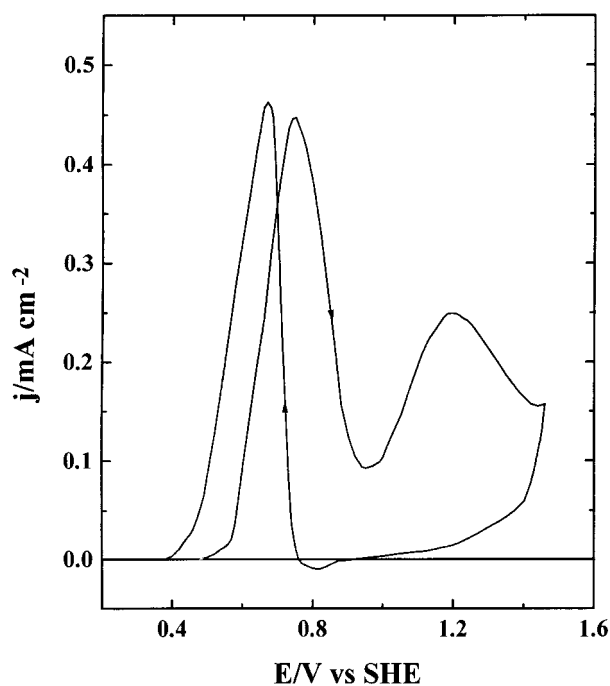


Fig. 1. Voltammogram for EG (0.1 M) oxidation on a Pt bead in 0.1 M HClO_4 . $|dE/dt| = 5 \text{ mV s}^{-1}$.

0.48 mA cm^{-2} and the descending part appears at 100 mV less positive potentials than the ascending part of the positive sweep. This hysteresis against the oxidation at the positive sweep is attributed to the blocking of the surface by strongly adsorbed CO [29, 30] resulting from the dissociative adsorption of EG on the platinum surface. This species is removed by oxidation at more positive potentials towards CO_2 by adsorbed oxygen species which thereafter forms a protective shield, thus allowing oxidation of EG during the negative-going sweep to take place at lower potentials.

Unlike smooth platinum, platinum electrodeposited in a polyaniline film allows electrooxidation of EG to begin at lower, by 100 mV, potentials. Figure 2 shows the quasi-steady state voltammogram of PANi/Pt (0.6 mg cm^{-2}) in the presence and absence of EG in a perchloric acid aqueous solution. In both voltammograms the positive potential limit was not extended beyond 1.02 V to avoid overoxidation and hydrolysis of the PANi film. The supporting electrolyte shows the typical behaviour of a polyaniline coated electrode in a perchloric acid solution. In the presence of EG the curve is different from that observed on the smooth metal. During the positive-going sweep oxidation commences at 0.35 V. The curve exhibits two peaks, one at 0.64 V (3.56 mA cm^{-2}) and a second at 0.77 V (3.11 mA cm^{-2}), which is not the second oxidation peak of PANi. The negative-going sweep also exhibits two overlapping peaks, at 0.59 V (2.14 mA cm^{-2}) and 0.66 V (2.23 mA cm^{-2}). The current densities are calculated after subtracting the background current and considering as electrode surface the geometric surface area of the supporting electrode. Hysteresis towards the oxidation of EG is

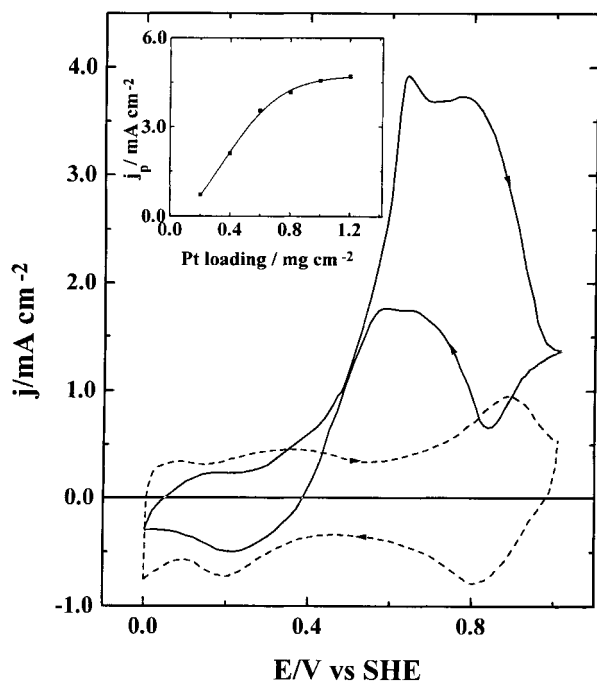


Fig. 2. Voltammograms obtained on a PAni/Pt (0.6 mg cm^{-2}) electrode in 0.1 M HClO_4 in the absence (---) and the presence (—) of EG 0.1 M . $|dE/dt| = 5 \text{ mV s}^{-1}$. The inset shows the plot of the current density of the first oxidation peak of EG vs platinum loading.

also observed here, but to a lower extent than in the case of smooth platinum.

The shape of the voltammogram obtained on platinum microparticles shows that ethylene glycol molecules begin to oxidize from potentials (peak at 0.64 V) where strongly adsorbed OH species are not yet formed. The second peak, which appears at 0.77 V , represents oxidation of EG species that remain adsorbed on platinum and of new EG molecules which approach and interact with the surface via the recently released sites. This oxidation is driven by the action of chemisorbed OH and O species. The appearance of the onset of EG electrooxidation on PAni/Pt at lower potentials than on smooth Pt is based on the fact that highly dispersed platinum is less susceptible to poisoning, that is mainly strongly adsorbed CO [26], formation [31].

Penetration and diffusion of EG through the polymer film appears to be a slow step and affects the whole mechanism. Under rotating conditions the height of the current peaks depends on the rotation rate. For low rotation rates ($5.2 < \omega < 104.7 \text{ rad s}^{-1}$) an increase is observed. For higher ω values, however, no further increase is observed and the electrode surface is easily poisoned as the degree of CO adsorption increases. Figure 3 shows the dependence of j^{-1} on $\omega^{-1/2}$ for low rotation rates and different film thicknesses. As expected, the intercept is proportional to the film thickness, showing that transport of EG through the film is a controlling factor and that the particles of platinum are not concentrated on the polymer-solution interface but dispersed in a three-dimensional manner in the

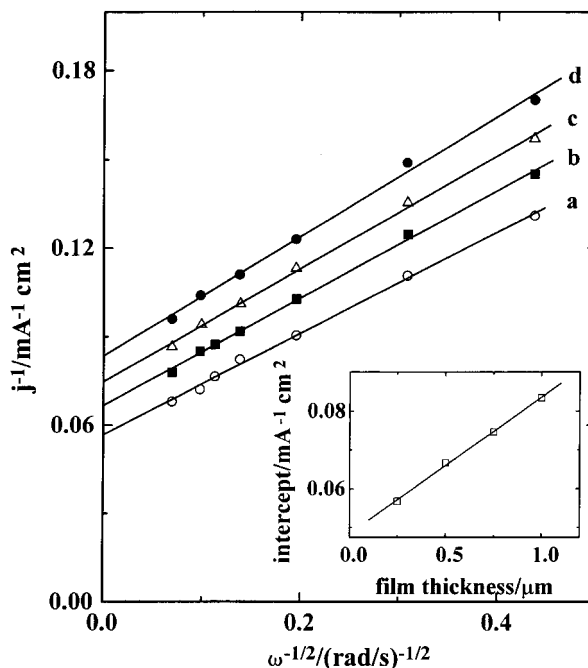


Fig. 3. Koutecky-Levich plots (j^{-1} vs $\omega^{-1/2}$) for the oxidation of EG (0.1 M) on a PAni/Pt (0.6 mg cm^{-2}) rotating disc electrode in 0.1 M HClO_4 for different PAni film thicknesses: (a) 0.25 , (b) 0.50 , (c) 0.75 and (d) $1.00 \mu\text{m}$.

polymer matrix, which is in line with earlier studies [13]. Information concerning the identification of the phases and the actual morphology of a PAni/Pt electrode was obtained using transmission electron microscopy.

Figure 4(a) shows a PAni/Pt electrode. Platinum exists in the form of very fine microparticles which

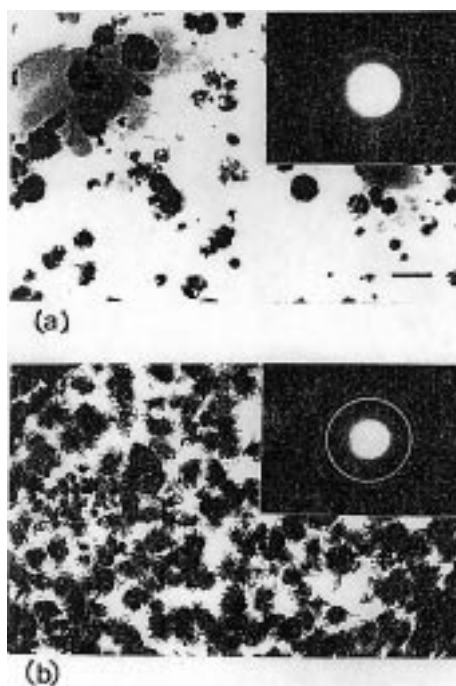


Fig. 4. TEM images of a PAni/Pt (a) and a PAni/Pt-Ru (b) electrode and the corresponding diffraction patterns (bar $\equiv 0.2 \mu\text{m}$ for both micrographs).

aggregate in groups three-dimensionally and are almost homogeneously dispersed over the polymeric matrix. Each group has a spherical-like shape and the distribution of its component microparticles becomes denser towards the centre of the sphere. The inset diffraction pattern certifies (Table 1) that the observed crystalline phase consists of Pt microcrystallites.

Studies [10, 32] using microparticulate electrodes have shown that the catalytic activity of such electrodes is a function, among others, of the mass electrodeposited and the size of the particles, factors which are definitely interdependent. Number, size and arrangement of the particles in space depend on, and thus can be controlled by, the conditions of metal electrodeposition. The activity of the electrode PANi/Pt for EG electrooxidation was examined for different platinum loadings. Changes in the platinum loading affect the oxidation current as they change the surface area of the electrode. Indeed, as shown in the inset of Fig. 2 current density increases with the mass of metal incorporated and reaches a maximum value of 4.71 mA cm^{-2} at 1.2 mg cm^{-2} . The observed decrease of the catalytic activity for higher loadings probably means that for these deposits the system exhibits a lower degree of dispersion.

3.2. EG electrooxidation on Pt-based multimetallic systems dispersed in polyaniline

The catalytic activity of the dispersed electrode is even more enhanced when instead of PANi/Pt, the multimetallic assemblies PANi/Pt–Ru, PANi/Pt–Sn and PANi/Pt–Ru–Sn are employed. Figures 5, 6 and 7 show the quasi-steady state voltammograms of Pt–Ru, Pt–Sn and Pt–Ru–Sn, respectively, in perchloric acid solution containing EG. In all cases the shape remains almost the same; two overlapping peaks in both directions. In the case of PANi/Pt–Ru, EG electrooxidation starts at the same potential as in the case of PANi/Pt. Yet the first maximum is found at less positive, by around 40 mV, potentials. The main difference in the behaviour of the two catalysts rests in the current values. The presence of ruthenium causes an increase by almost double for the forward scan and more than triple for the reverse. In the case of PANi/Pt–Sn a much lower increase in the current

Table 1. d_{hkl} values of Pt taken from PDF [34], in comparison with the measured values (d_{obs}) from the diffraction pattern

$h k l$	d/nm	d_{obs}/nm
111	0.2265	0.226
200	0.1962	0.197
220	0.1387	0.139
311	0.118 26	0.118
222	0.113 25	
400	0.098 08	
331	0.090 00	
420	0.087 73	
422	0.080 08	

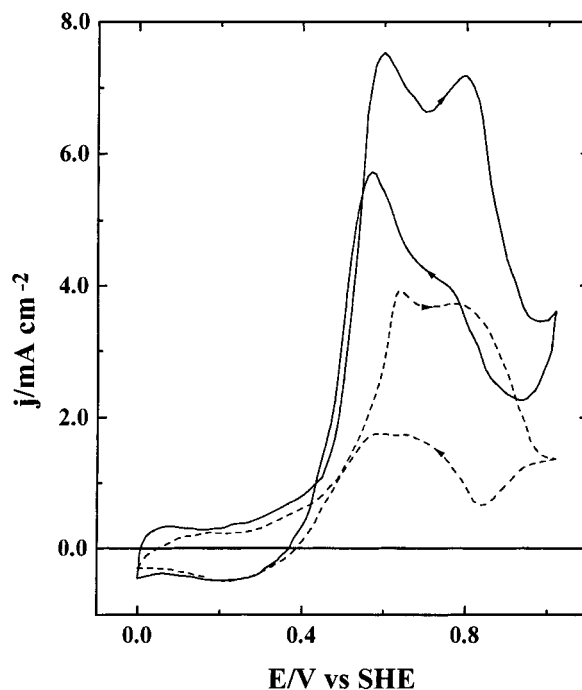


Fig. 5. Voltammograms for EG (0.1 M) oxidation on a PANi/Pt–Ru (0.6 mg cm^{-2}) (—) and a PANi/Pt (0.6 mg cm^{-2}) (---) electrode in 0.1 M HClO_4 . $|dE/dt| = 5 \text{ mV s}^{-1}$.

but a significant decrease in the onset potential of EG electrooxidation are observed. The oxidation reaction starts at 0.2 V. In the case of PANi/Pt–Ru–Sn, the voltammogram exhibits characteristics from both PANi/Pt–Ru and PANi/Pt–Sn electrodes. The voltammetric behaviour is a combination of these two systems. Thus, EG oxidation starts at 0.28 V and the first peak of the positive-going sweep appears at

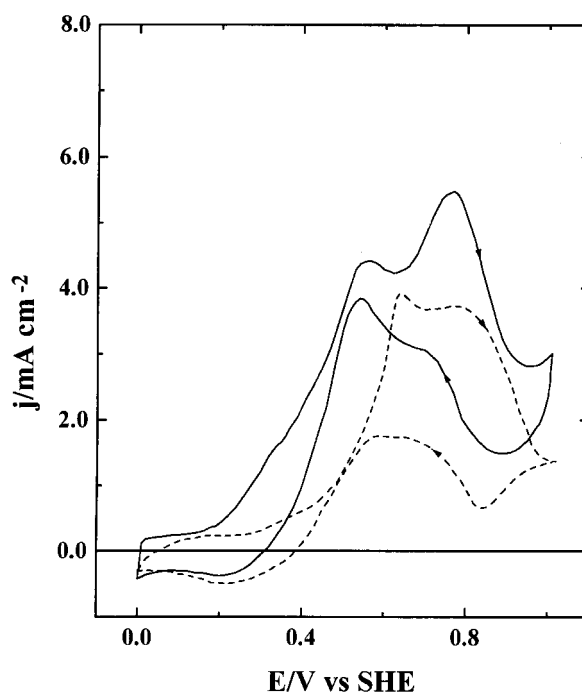


Fig. 6. Voltammograms for EG (0.1 M) oxidation on a PANi/Pt–Sn (0.6 mg cm^{-2}) (—) and a PANi/Pt (0.6 mg cm^{-2}) (---) electrode in 0.1 M HClO_4 . $|dE/dt| = 5 \text{ mV s}^{-1}$.

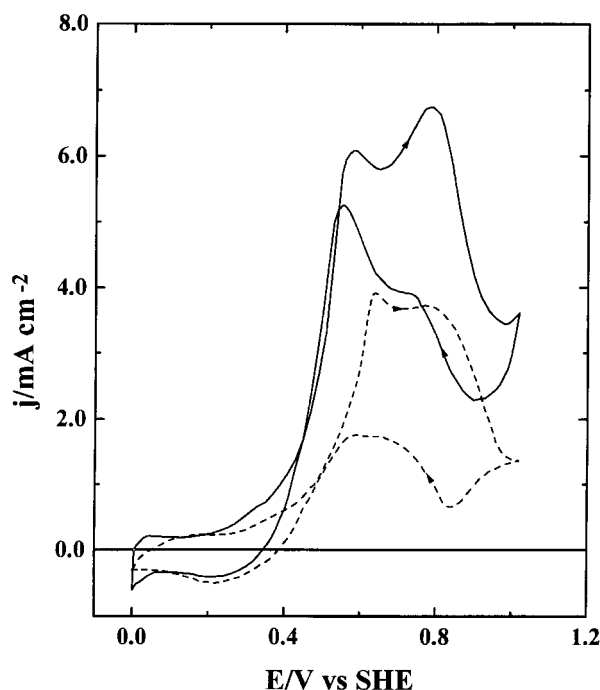


Fig. 7. Voltammograms for EG (0.1 M) oxidation on a PANi/Pt-Ru-Sn (0.6 mg cm^{-2}) (—) and a PANi/Pt (0.6 mg cm^{-2}) (- - -) electrode in 0.1 M HClO_4 . $|dE/dt| = 5 \text{ mV s}^{-1}$.

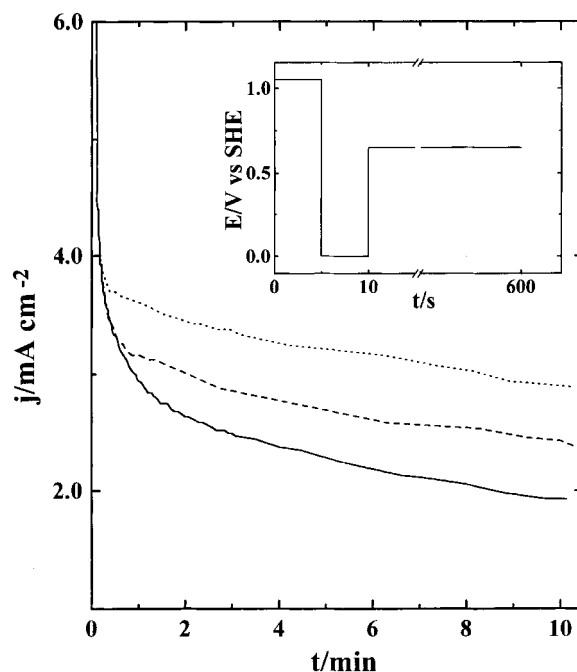


Fig. 8. Time dependence of the total current of the first oxidation peak of EG (0.1 M) on PANi/Pt and PANi/Pt-Ru (—), PANi/Pt-Ru-Sn (- - -) and PANi/Pt-Sn (⋯⋯). In all cases the total metallic mass incorporated is 0.6 mg cm^{-2} .

0.58 V (5.74 mA cm^{-2}) and the second at 0.77 V (6.11 mA cm^{-2}).

Earlier studies on bimetallic assemblies [4, 33] have shown that the oxygen species, which are necessary for the oxidation of organic molecules on platinum, start to form at very low potentials on Ru or Sn sites and readily react with the carbon adsorbed species of Pt sites. This bifunctional mechanism is responsible for the decrease in the overpotential of ethylene glycol electrooxidation observed mainly in the case of PANi/Pt-Sn in which the hysteresis phenomenon, observed in all other catalysts examined, disappears. As regards the large increase in current in PANi/Pt-Ru electrocatalysts, transmission electron microscopy studies (Fig. 4(b)) reveal that in PANi/Pt-Ru assemblies the metallic microparticles exhibit a finer dispersion and thus the same metallic mass leads to a larger electrode surface area. It should be noted that the only phase detected is Pt and no Ru rings are observed in the corresponding diffraction patterns. One explanation might be that Ru exists in the form of adatoms on Pt microcrystallites or that the condensed mass of Ru crystallites is too low to be detected.

The long-term stability of the electrodes employed was checked with the time dependence of the current at the first peak maximum of the positive-going sweep. Figure 8 shows that the PANi/Pt-Sn electrode, among the used multimetallic electrodes, is the most stable electrocatalyst. Within the first 10 min there is only a 23% decrease in the value of the observed current, whereas for PANi/Pt and PANi/Pt-Ru this decrease amounts 49%. Such an observation verifies that the addition of Sn as a second or third metal reduces poison formation.

The stability of the electrode was also tested against storage and time of usage. It was found that the catalytic activity of freshly prepared electrodes was only slightly better than that of the same electrodes after having been used and stored overnight in aqueous solution containing 0.1 M HClO_4 . Under rotating conditions the catalytic activity remained almost constant even after repetitive use, indicating that intense stirring does not cause significant damage to the polymer film.

3.3. Influence of heavy metal ad-atoms deposited at underpotentials

The influence of heavy metal adatoms deposited at underpotentials on the oxidation of EG on Pt microparticles was also studied. According to the literature [1], smooth Pt modified by underpotential monolayers of Pb, Tl and Bi is a better catalyst than pure Pt towards EG electrooxidation in acid solutions.

When platinum is dispersed in polyaniline, however, Tl and Bi adatoms inhibit EG oxidation. Lead underpotential deposition has a positive effect on the catalytic activity of Pt (Fig. 9) only when Pt is electrodeposited on PANi films from a solution also containing a lead salt, as described in the experimental section. The current of the first peak of the anodic sweep and the last one during the cathodic sweep become almost double. As bulk lead cannot be deposited at the potential employed (0.1 V), it is very possible that Pb atoms are incorporated in the platinum particles due to their underpotential deposition taking place during the electrodeposition process.

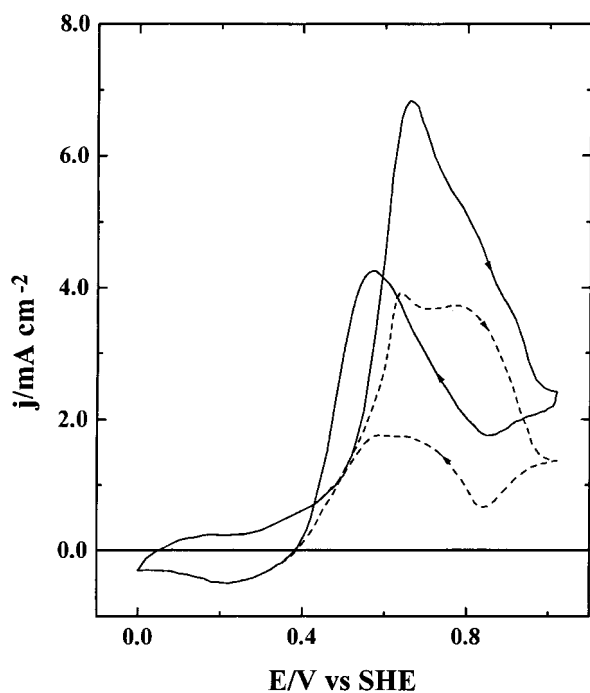


Fig. 9. Voltammograms for EG (0.1 M) oxidation on a PAAni/Pt-Pb (0.6 mg cm^{-2}) (—) and a PAAni/Pt (0.6 mg cm^{-2}) (---) electrode in 0.1 M HClO_4 . $|dE/dt| = 5 \text{ mV s}^{-1}$.

Lead atoms present in the surface together with platinum inhibit chemisorption of weakly adsorbed species, according to the third body effect, and enhance the catalytic activity of the electrode.

Acknowledgements

This work was performed within a research project (PENED Oct. 1996, code 1706) supported by the General Secretariat of Research and Technology, Greece.

References

- [1] G. Kokkinidis and D. Jannakoudakis, *J. Electroanal. Chem.* **133** (1982) 307.
- [2] F. Kadirgan, B. Beden and C. Lamy, *ibid.* **136** (1982) 119.
- [3] G. Pierre, A. Ziade and M. El Kordi, *Electrochim. Acta* **32** (1987) 601.

- [4] M. Watanabe and S. Motoo, *J. Electroanal. Chem.* **60** (1975) 267.
- [5] M. M. P. Janssen and J. Moolhuysen, *Electrochim. Acta* **21** (1976) 861.
- [6] E. Herrero, J. M. Feliu and A. Aldaz, *J. Electroanal. Chem.* **368** (1994) 101.
- [7] M. S. Ureta-Zanartu, C. Yanez, M. Paez, G. Reyes, *ibid.* **405** (1996) 159.
- [8] J. P. I. Souza, F. J. Botelho Rabelo I. R. de Moraes, F. C. Nart, *ibid.* **420** (1997) 17.
- [9] G. Tourillon and F. Garnier, *J. Phys. Chem.* **88** (1984) 5281.
- [10] W.-H. Kao and T. Kuwana, *J. Am. Chem. Soc.* **106** (1984) 473.
- [11] D. E. Bartak, B. Kazee, K. Shimazu and T. Kuwana, *Anal. Chem.* **58** (1986) 2756.
- [12] L. Coche and J.-C. Moutet, *J. Am. Chem. Soc.* **109** (1987) 6887.
- [13] K. M. Kost, D. E. Bartak, B. Kazee and T. Kuwana, *Anal. Chem.* **60** (1988) 2379.
- [14] S. Holdcroft and B. Lionel Funt, *J. Electroanal. Chem.* **240** (1988) 89.
- [15] P. O. Esteban, J.-M. Léger, C. Lamy and E. Genies, *J. Appl. Electrochem.* **19** (1989) 462.
- [16] M. Gholamian and A. Q. Contractor, *J. Electroanal. Chem.* **289** (1990) 69.
- [17] M. Ulmann, R. Kostecki, J. Augustynski, D. J. Strike and M. Koudelka-Hep, *Chimia* **46** (1992) 138.
- [18] A. Leone, W. Marino and B. R. Scharifker, *J. Electrochem. Soc.* **139** (1992) 438.
- [19] C. S. C. Bose and K. Rajeshwar, *J. Electroanal. Chem.* **333** (1992) 235.
- [20] C. C. Chen, C. S. C. Bose and K. Rajeshwar, *ibid.* **350** (1993) 161.
- [21] H. Laborde, J.-M. Léger and C. Lamy, *J. Appl. Electrochem.* **24** (1994) 219.
- [22] W. T. Napporn, H. Laborde, J.-M. Léger and C. Lamy, *J. Electroanal. Chem.* **404** (1996) 153.
- [23] W. T. Napporn, J.-M. Léger and C. Lamy, *ibid.* **408** (1996) 141.
- [24] S. Ye, A. K. Vijh and L. H. Dao, *ibid.* **415** (1996) 115.
- [25] G. Inzelt and G. Horanyi, *Acta Chim. Acad. Sci. Hung.* **101** (1979) 229.
- [26] J. M. Orts, A. Fernandez-Vega, J. M. Feliu, A. Aldaz and J. Clavilier, *J. Electroanal. Chem.* **290** (1990) 119.
- [27] J. C. LaCroix and A. F. Diaz, *J. Electrochem. Soc.* **135** (1988) 1457.
- [28] D. E. Stilwell and S.-M. Park, *ibid.* **135** (1988) 2491.
- [29] F. Hahn, B. Beden, F. Kadirgan and C. Lamy, *J. Electroanal. Chem.* **216** (1987) 169.
- [30] P. A. Christensen and A. Hamnett, *ibid.* **260** (1989) 347.
- [31] B. Beden, F. Hahn, J.-M. Léger, C. Lamy, C. L. Pedriel, N. R. De Tacconi, R. O. Lezna and A. J. Arvia, *ibid.* **301** (1991) 129.
- [32] A. Yassar, J. Roncali and F. Garnier, *ibid.* **255** (1988) 53.
- [33] N. M. Markovic, H. A. Gasteiger, P. N. Ross Jr, X. Jiang, I. Villegas and M. J. Weaver, *Electrochim. Acta* **40** (1995) 91.
- [34] J. V. Smith (ed.), 'X-ray Powder Data Files' (1960) (American Society for Testing Materials) card no. 4-802.